High Quantum Efficiency of (Au/n-SnO_2/p-PSi/c-Si/Al) solar cell after annealing of Nd:YAG laser

The 5th International scientific Conference on Nanotechnology& Advanced Materials Their Applications (ICNAMA 2015) 3-4 Nov, 2015

Dr. Firas Sabeeh Mohammed
College of Science, Al- Mustansiriyah University/Baghdad.
Dr. Ban Rashid Ali
College of Science, Al- Mustansiriyah University/ Baghdad.
Bahaa Jawad Alwan
College of Science, Al- Mustansiriyah University/ Baghdad.
Zahra Sabah Rashid
College of Science, Al- Mustansiriyah University/ Baghdad.

Abstract

Transparent and conducting SnO_2 thin film has been produced on (quartz and porous silicon) substrates using rapid photothermal oxidation of pure Sn in air at 600 ^oC oxidation temperature and different oxidation time. The structural properties and scan electron microscope of the prepared films were studied. The photovoltage properties of a Au/n-SnO_2/p-PSi/c-Si solar cell are investigated under irradiation of Nd:YAG laser pulses. The porous Si layer is synthesized on a single crystalline p-type Si using electrochemical etching in aqueous hydrofluoric acid at a current density of 25 mA/cm^2 for a 30-min etching time. The structure of the porous layer is investigated using scan electron microscope. The photovoltage properties are found to be dependent on the laser fluencies.

Keywords: Tin oxide, rapid thermal oxidation, Electrochemical etching, Au/n-SnO_2/p-PSi/c-Si solar cell.

كفاؤة كمية عالية للخلية الشمسية (Au/n-SnO_2/p-PSi/c-Si/Al) بعد التلدين

الخلاصة:

اكاسيد شفافة موصلة SnO_2 محضرة على قواعد مختلفة باستخدام تقنية الاكسدة الحرارية السريعة لمعدن القصدير بالهواء عند درجة حرارة اكسدة 600 ^oC وازمان اكسدة مختلفة. الخصائص التركيبية تم دراستها في هذا البحث. تم تحضير طبقة اليليكون المسامي في هذا البحث باستخدام سليكون نوع p-type Si بمحلول حامض الهايدروفلوريك عند كثافة تيار مقدارها 25 mA/cm^2 لمدة 30-min. حيث تم قياس الخصائص الفولتائية للنبيطة المصنعة بعد اجراء عملية التلدين كخلية شمسية حيث اظهرت كفاؤة عالية جدا بعد التلدين.

INTRODUCTION

Tin dioxide (**SnO_2**) with the rutile structure is an n-type semiconductor with a wide band gap ~3.6 eV. The structural characteristics of polycrystalline tin oxide thin films are of great importance in various applications such as chemical sensors, solar cells, and optoelectronic devices [1, 2]. SnO_2 thin films have been fabricated using different techniques including dc gas discharge activating reaction evaporation technique [3], electron beam evaporation [4], rf sputtering [5-7], Plasma Enhanced Chemical Vapor Deposition [8], hydrothermal [9] and chemical vapor deposition [1, 10, 11]. One of the major challenges in synthesizing SnO_2 thin

films is the control over stoichiometry. Since most depositions are carried out in high vacuum condition at high temperatures, the SnO_2 films obtained are nonstoichiometric and frequently consist of metastable phases such as SnO and Sn_3O_4 [12]. The existence of these metastable phases and crystal defects will strongly affect the properties of the films [12, 13]. Therefore, a post deposition annealing in the air is necessary to obtain the stoichiometric SnO_2 phase with the rutile structure. However, the microstructure of the resulting SnO_2 films is mainly controlled by the annealing process and a number of crystal defects are frequently observed in these films. The structure of the SnO_2 material in its bulk form is tetragonal rutile with lattice parameters a = b = 4.737 Å and c = 3.816 Å. However in thin film form, depending on the deposition technique its structure can be polycrystalline or amorphous. The grain size is typically 200–400 Å, which is highly dependent on deposition technique, temperature, doping level etc. SnO_2 films close to stoichiometric condition have low free carrier concentration and high resistivity, but non-stoichiometric SnO_2 films have high carrier concentration, conductivity and transparency. This comes about from an oxygen vacancy in the structure so that the formula for the thin film material is $SnO_2{-}x$, where x is the deviation from stoichiometry [14]. In the present work, we demonstrate the effect of pulsed Nd-Yag laser irradiation at different fluencies of 20, 30, 40, and 50 mJ/cm^2 in air at room temperature on the performance of a Au/SnO_2/PSi/c-Si device for solar cell fabricated by electrochemical etching.

Experimental Work

High purity of tin (Sn) thin film was deposited on (quartz and p-type PSi single crystal (111) silicon substrates) using thermal evaporation technique at room temperature under vacuum pressure of 10^{-6} Torr. Electrochemical anodization was performed in dark to produce porous Si layers on polished p-type, single crystal (111) oriented Si wafers with a resistivity of 10 Ω–cm and a thickness of ~ 508±5 μm, using a 1:4 mixture of 48 % HF: 99% ethanol as an electrolyte. Ethanol was added to the HF solution in order to improve the wettability of the acid, allow the diffusion of F ions into pores, improve the PSi layer uniformity by removing the hydrogen bubbles, help moisten the silicon surface, and improve reproducibility [15]. However, the addition of ethanol to HF eliminates hydrogen and ensures complete infiltration of HF solution within the pores which further improves the uniform distribution of porosity and thickness. Initially, the Si wafers were cleaned successively in a sonicating bath with CCl_4, toluene, acetone, ethyl alcohol and 18.5 M-cm deionized water. The anodization was carried out with the distance between the Si substrate to the Pt counter electrode fixed at ~ 2.5 cm, using a current density of 25 mA/cm^2 for a fixed time of 30 min. The wafer and platinum cathode were placed in a Teflon jig, schematically illustrated in figure (1). As shown in figure (1), the base and the cap of the electrochemical etching cell were made with SS 320 metal. Silicon wafer was placed inside the base and sealed with an O-ring and exposed to the electrolyte. The surfaces of Si substrate and Pt cathode were kept parallel to each other and the current flow in the etchant was normal to the wafer surface. After the anodization, the PSi layers were dried in the following way to reduce the capillary stress using pentane, which has very low surface tension and no chemical reactivity with the PSi layer. The samples were rinsed first with pentane, then with 98 % methanol and finally with deionized water (18.5 M-cm). Next, the samples were dried at about 60 ^oC on a hot plate rather than drying in the N_2 nozzle in order to avoid cracking and peeling of the

PSi layer. The resistivity and type of conductivity of the Si substrates were measured by using four point probe (FPP) technique. SnO_2 film was obtained with aid of rapid photo-thermal oxidation system with halogen lamp as oxidation source. The oxidation condition used to form SnO_2 film was 600 ^oC and different oxidation times. The system used to prepare the oxide film; where a quartz tube of 3 cm diameter with two open ends was used to ensure the flowing of air through it. The source of dry oxygen was used. 650 W halogen lamps were used to provide light and heat radiation and a variable power supply to control the output power. A k-type thermocouple was used to monitor samples temperature. The silicon sample was used as substrate for TCO's/PSi heterojunction. Ohmic contacts were fabricated by evaporating 99.999 purity aluminum wires for back contact and 99.999 pure gold were used as front contact through special mask using Edwards coating system . A boat of tungsten was used to include the evaporated source. A pulsed Nd-YAG laser system type (Guangzhou Huafei Tongda Technology Co., China), providing pulses at (1064) nm wavelength and a pulse duration of 10 ns, was used for treatment of a Au/SnO_2/PSi/c-Si at different fluences of 20, 30, 40, and 50 mJ/cm^2 in air at room temperature.

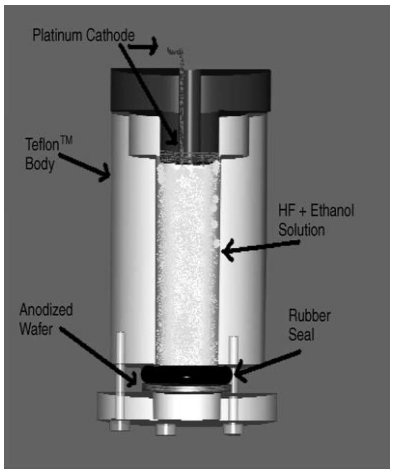

Figure (1): Schematic illustration of the porous silicon etching setup.

Results and Discussion

XRD-diffraction:

The structure and lattice parameters of SnO_2 films were analyzed by a LabX XRD 6000 SHIMADZU XR – Diffractometer with Cu Kα radiation of (voltage 30 kV, current 15 mA, scanning speed = 4°/min). Figure (2) shows the diffraction pattern for samples prepared at oxidation temperature 600 ^oC and different oxidation time. The XRD patterns at oxidation time of 60 sec are shown in figure (2) (a). It is shows that the peaks appeared at $2\theta=33.8436^\circ$ and $2\theta= 34.0896^\circ$ are corresponding to the diffraction from (101) planes which are related to the formation of SnO_2 films. At 90 sec oxidation time and 600 ^oC oxidation temperature as figure (2) (b) show that the structures of films are clearly improved where a significant increase in peak intensity at (101) plane can be attributed to the improvement in the structural order can also be attributed to the increase in the SnO_2 film density, which results in demonstrated of (101) SnO_2 peak rather than other peak. This indicates the formation of nearly

stoichiometry SnO_2 films. The intensities of these peaks reduce with the increasing of oxidation time up to 120 sec as shown in figure (2) (c). The results below ensure that the optimum value of oxidation temperature is 600 ^oC and oxidation time is 90 sec. The deviation in XRD peak of the film with respect to the standard ASTM data is attributed to the mechanical micro stress produced by different sources like impurities, defects and vacancies reside in the film structure. Results at higher oxidation time 140 sec and at the same oxidation temperature are shown in figure (2) (d), which recognizes the peaks at $2\theta=33.9813^\circ$ in the spectra of SnO_2 film corresponding to the reflection from (101) plane. The presence of sharp peak (in all deprogram) indicates that all films are polycrystalline in nature with a tetragonal structure and in accordance with data reported in literature [1-3]. Table (1) shows the effect of oxidation times on the XRD characteristics evaluated from the diffrograms. In the case of tetragonal structure which is the ruling form for SnO_2 thin films, the lattice constants are $a=b\neq c$ as shown in Table (2). These constants change with structural change caused by the different parameters such as deposition technique, doping, substrate, etc., and the lattice constant can be found by measuring different values of (d) not less than two or three or four times of x-ray spectrum by using the formula [7]:

$$\frac{1}{d^2}=\frac{(h^2+k^2)}{a^2}+\frac{l^2}{c^2} \quad \ldots (1)$$

Where

h, k, l are the Miller indices of the lattice plane. The values of lattice constants for SnO_2 films prepared at different oxidation temperature and oxidation time have been listed in Table (2). The grain size (D) is calculated using the Scherrer formula from the full-width half-maximum (FWHM) (β) [8]:

$$D=\frac{K\lambda}{\beta\cos\theta} \quad \ldots(2)$$

Where

λ is the wavelength of the X-ray used, β is the FWHM, D is the grain size value and θ is half the angle between incident and the scattered X-ray beams. The (D) values listed in the Table 3. It shows that grain size of the films is increased with increasing of oxidation time up to (90 sec).The intense and sharp peaks in XRD pattern reveal the good crystallinity of the films and also confirm the stoichiometric nature of SnO_2 films.

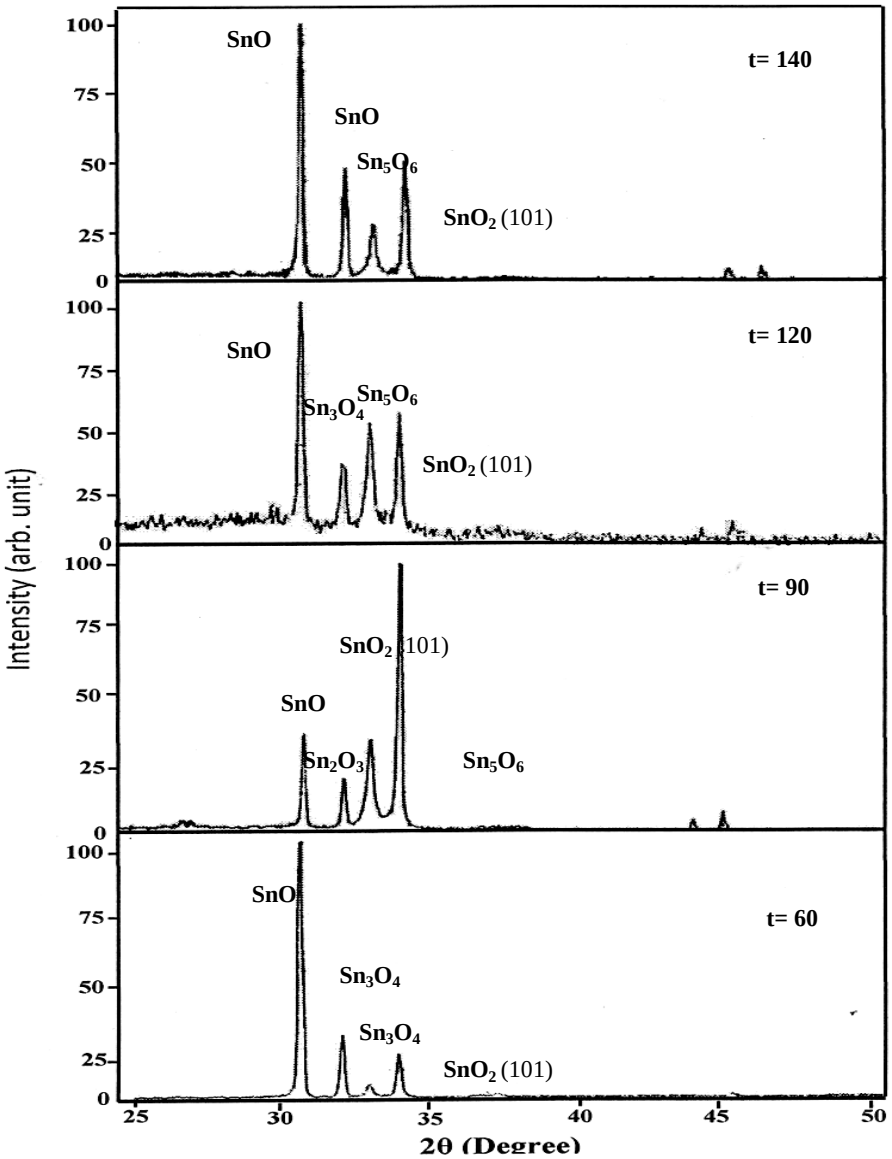

Figure (2): X-Ray diffraction patterns for SnO_2 thin films prepared quartz substrate at different oxidation time and 600 ^oC.

Table (1) XRD patterns characteristics of SnO_2 films at various oxidation times.

Deposition condition	(2Θ)°	I/I_1 XRD	d (Å) XRD	(h k l)	(2Θ)° ASTM	I/I_1 ASTM	d (Å) ASTM	Type
t= 60 sec	30.8484	100	2.89626	---	30.916	90	2.89	SnO
T= 600 ^oC	32.2340	25	2.77486	---	32.315	50	2.768	Sn_3O_4
	33.1044	8	2.70386	---	33.014	50	2.711	Sn_3O_4

	34.0896	10	2.62794	101	34.061	80	2.63	**SnO_2**
t=90 sec T= 600 ^oC	30.7698	31	2.90348	101	30.807	80	2.90	**SnO**
	32.7901	6	2.72906	030	32.964	30	2.715	**Sn_2O_3**
	33.0188	30	2.71068	---	33.026	30	2.7100	**Sn_5O_6**
	34.0027	100	2.63446	101	34.061	80	2.63	**SnO_2**
t=120 sec T= 600 ^oC	30.9004	100	2.89151	---	30.916	90	2.89	**SnO**
	32.3045	26	2.76896	---	32.315	50	2.768	**Sn_3O_4**
	33.1776	42	2.69806	---	33.026	30	2.7100	**Sn_5O_6**
	34.1664	45	2.62221	101	34.195	80	2.62	**SnO_2**
t=140 sec T= 600 ^oC	30.7550	100	2.90485	101	30.807	80	2.90	**SnO**
	32.1293	40	2.78366	021	32.172	40	2.78	**SnO**
	33.0054	18	2.71175	---	33.026	30	2.7100	**Sn_5O_6**
	33.9813	46	2.63607	101	33-928	63	2.64	**SnO_2**

Table (2) Lattice constants as a function of oxidation temperature and oxidation time of SnO_2 thin film.

Deposition condition	investigated line	TYPE	Lattice (a) Å	Lattice (c) Å
t=60 sec, T= 600 ^oC	101	SnO_2	4.706	3.168
t=90 sec, T= 600 ^oC	101	SnO_2	4.717	3.175
t=120 sec, T= 600 ^oC	101	SnO_2	4.695	3.161
t=140 sec, T= 600 ^oC	101	SnO_2	4.720	3.177
ASTM	101	SnO_2	4.750	3.198

Table (3) Grain size of SnO_2 Thin Film.

Deposition condition	investigated line	TYPE	β (degree)	Grain Size (D) nm
t=60 sec, T= 600 ^oC	101	SnO_2	0.1712	50.7169
t=90 sec, T= 600 ^oC	101	SnO_2	0.1544	56.2223
t=120 sec, T= 600 ^oC	101	SnO_2	0.1945	44.6505
t=140 sec, T= 600 ^oC	101	SnO_2	0.1557	55.7497

Scan electron microscope (SEM):

Surface morphologies obtained through Scanning Electron Microscope (SEM) study carried out by (Hitachi FE-SEM model S-4160, Japan) in University of Tehran at 15 kV of SnO_2 films prepared at oxidation temperature 600 ^oC and different oxidation times. SEM micrograph shows that surface of SnO_2 thin films are smoother as shown in figure (3) (a, b, c and d). The films consist of small particles distributed on the surface that shows nanostructure properties. The structure is polycrystalline with very fine pores distributed fairly uniformly on the film surface. We can observe a dense granular structure. The grains have different shapes and sizes. The grain size found using SEM is smaller than those derived from X-ray diffraction. From SEM observations given by figure (3), we note that the average grain size is comparable to the film thickness which is less than 100 nm.

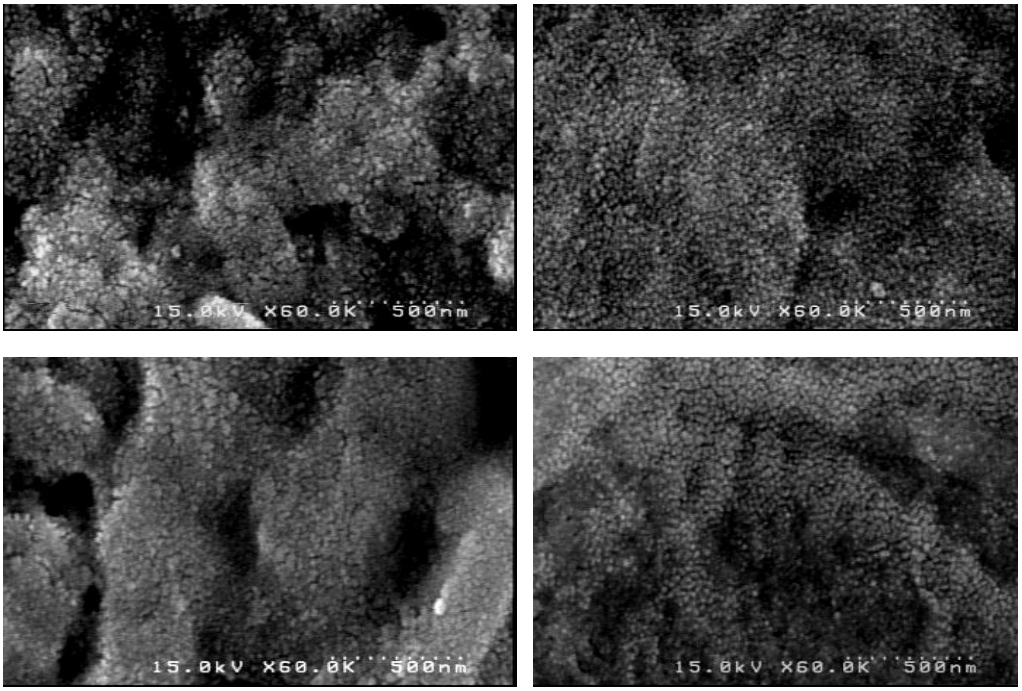

Figure (3) Scan electron microscope of SnO_2 film prepared on quartz substrate at 600 ^oC and oxidation time (a) 60 sec, (b) 90 sec, (c) 120 sec and (d) 140 sec.

Figure (4) illustrates the SEM image of the PSi layer formed on the p-type c-Si (111) sample grown at current density of 25 mA/cm^2 for a fixed time of 30 min. The surface morphology of the structures in SEM plan view for the porous silicon structures, respectively. The array of void spaces (dark) in silicon matrix (bright) can be seen clearly in the plan view SEM image [16, 17]. The morphology of the structures shows that the electrochemical etching is done uniformly on the surface and created the granular structure in a spherical shape. Large number of pores distributed in all direction can be observed figure (4) (a). Pores with sphere-like

appearances were evidently randomly distributed on the PSi surface. A modest density of pores was observed, and porosity was approximately 85%.The average pore diameter for the PSi layer formed on the p-type c-Si (111) wafers was 26.41 nm.

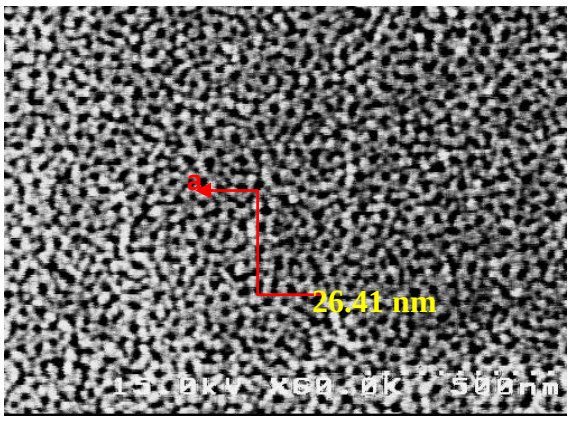

Figure (4): (a) Scan electron microscope of porous silicon.

The current-voltage characteristics of the solar cells were examined under 100 mW/cm^2 illumination. The relationship between Isc and Voc as a function of load resistance could be recognize in figure (5) (a, b). The efficiency of the Au/SnO_2/PSi/c-Si device has been measured in five cases for comparison at different pulsed Nd-Yag laser irradiation fluencies of 20, 30, 40, and 50 mJ/cm^2 in air at room temperature. It value found to be (2, 3, 5.1, 6.4 and 8.3) respectively, the improved in value of Quantum efficiency (QE) after irradiation cases is related to the reflected of light rays from one side inside the key hall surface merely to strike another, resulting in an improved probability of absorption, and therefore reduced reflection comparing to the crystalline silicon surface [21]. Also due to the absorption phenomena in the surface oxide layer and at the Au/SnO_2/PSi/c-Si junction that formed between SnO_2 nanostructure thin film and porous silicon, beside that, the interfacial porous silicon oxide ($Psio_2$) layer between porous silicon (PSi) itself and metal oxide SnO_2 play a significant role in enhanced the properties, science it has been found that the porous silicon could be oxidized at high temperatures forming an porous oxide layer. Heating of porous silicon to high temperature in a strongly oxidation ambient leads to vary rapid oxidation of the structure. Rapid Thermal Oxidation of porous silicon makes it suitable as dielectric layer for any electronic device. Most of its applications involve the formation of stable SiO_2 layers obtain by a simple technological process like thermal oxidation of porous Si at high temperature is conveniently carried out by the use of rapid thermal oxidation (RTO); involving transient heat of oxygen ambient so that careful control of the potential rapid surface reaction can be maintained. The results (Table 4) also show that the conversion efficiency and fill factor of the solar cell using the following equation: [22]

$$\eta = \frac{P_m}{P_i} = \frac{I_m V_m}{P_i} \qquad \ldots(3)$$

Where
Pm and Pin are the output and incident powers, respectively. The fill factor (FF) was calculated by equation (6): [22]

$$FF = \frac{I_m V_m}{I_{sc} V_{oc}} \quad \ldots(4)$$

Table (4): The obtained results from the solar cell measurements.

Solar cells	I_m (mA)	V_m (mV)	I_{sc}(mA)	V_{oc}(mV)	FF%	η%
Au/SnO_2/PSi/c-Si	14	146.6	12.5	238.7	0.68	2
20 mJ/cm^2	15.2	201.5	16	262	0.73	3
30 mJ/cm^2	23	224.1	21.7	295	0.8	5.1
40 mJ/cm^2	27	238.7	25.8	320	0.78	6.4
50 mJ/cm^2	32	262	29.8	340	0.82	8.3

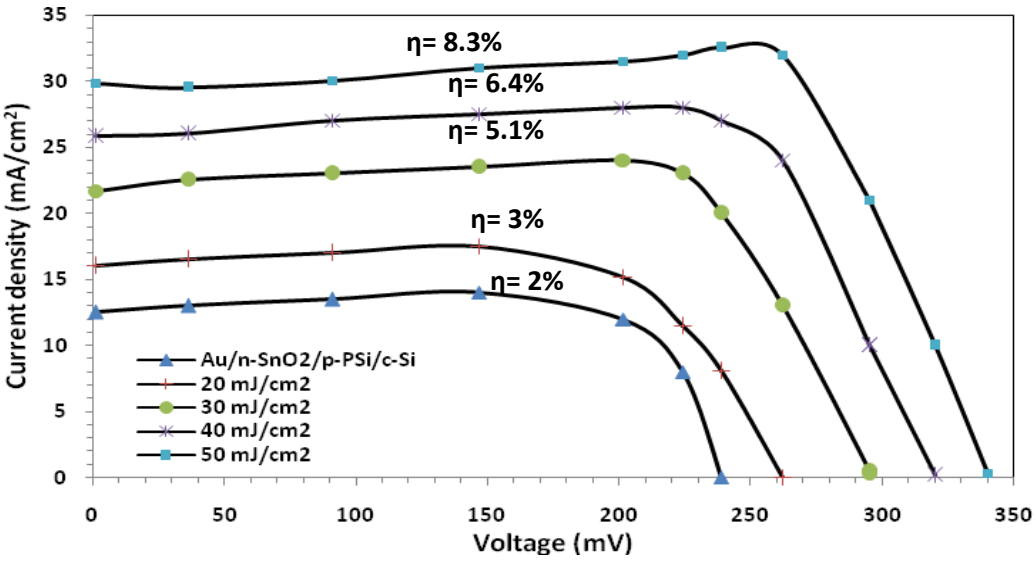

Figure (5): I-V characteristics of solar cells Au/SnO_2/PSi/c-Si devices at different pulsed Nd-Yag laser irradiation fluencies of 20, 30, 40, and 50 mJ/cm^2 in air at room temperature.

Conclusions

Transparent and conducting SnO_2 thin film has been produced on (quartz and porous silicon) substrates using rapid photothermal oxidation of pure Sn in air at 600 ^oC oxidation temperature and different oxidation time. The structural properties and scan electron microscope of the prepared films were studied. The photovoltage properties of the Au/n-SnO_2/p-PSi/c-Si solar cells were investigated.

References

[1] T. J. Stanimirova, P. A. Atanasov, I. G. Dimitrov, A. O. Dikovska" Investigation on the structural and optical properties of tin oxide films grown by pulsed laser deposition" Journal of Optoelectronics and Advanced Materials, Vol. 7, No. 3, June (2005), pp: 1335 – 1340.

[2] Novinrooz, Abdoljavad; Sarabadani, Parvin; Garousi, Javad "Characterization of Pure and Antimony Doped SnO_2 Thin Films Prepared by the Sol-Gel Technique" Iran. J. Chem. Chem. Eng. Vol. 25, No.2, (2006), PP: 31-38.

[3] Shengyue Wang, Wei Wang, Qingxiang Hu, Yitai Qian, "Surface modification of tin oxide ultrafine particle thin films", Materials Research Bulletin, Vol. 35, (2000), pp: 1235–1241.

[4] Sardar M. Ayub Durrani "Biasing Voltage Dependence of Sensitivity of Electron Beam Evaporated SnO_2 Thin Film CO Sensor" Sensors, Vol.6, (2006), pp: 1153-1160.

[5] K. Zakrzewskaa, M. Radeckaa, J. Przewoz´nika, K. Kowalskia, P. Czuba "Microstructure and photoelectrochemical characterization of the TiO_2–SnO_2 system" Thin Solid Films, 490, (2005), pp: 101 – 107.

[6] Young-ll Kim, Joo-Byoung Yoon, Jin-Ho Choy, Guy Campet, Didier Camino, Josik Portier, and Jean Salardenne" Rf sputtered SnO_2, Sn-doped In_2O_3 and Ce-doped TiO_2 films as transparent counter electrodes for electrochromic window" Bull. Korean Chem. Soc. Vol. 19, No. 1, (1998), pp: 107-109.

[7] Divya Haridas, Arijit Chowdhuri, K. Sreenivas, and Vinay Gupta " Enhanced LPG response characteristics of SnO_2 thin film based sensors loaded with Pt clusters" International journal on smart sensing and intelligent systems, Vol. 2, No. 3, (2009), pp: 503-514.

[8] Jeong-Hoon Leea, Gun-Eik Janga, Dae-Ho Yoonb and Sang-Hee Sonc "Effect of deposition temperature on electro-optical properties of SnO_2 thin films fabricated by a PECVD method" Journal of Ceramic Processing Research. Vol. 8, No. 1, (2007), pp: 59-63.

[9] U. Pal, A. Pérez-Centeno, and M. Herrera-Zaldívar "Cathodoluminescence defect characterization of hydrothermally grown SnO_2 nanoparticles" J. Appl. Phys. Vol. 103, No. 064301, (2008), pp: 1-6.

[10] R.G. Dhere, H.R. Moutinho, S. Asher, D. Young, X. Li, R. Ribelin, and T. Gessert" Characterization of SnO_2 Films Prepared Using Tin Tetrachloride and Tetra Methyl Tin Precursors" National Renewable Energy Laboratory, October (1998), pp: 1-6.

[11] D.M. Qu, P.X. Yan, J.B. Chang, D. Yan, J.Z. Liu, G.H. Yue, R.F. Zhuo, H.T. Feng" Nanowires and nanowire–nanosheet junctions of SnO_2 nanostructures" Materials Letters, Vol.61, (2007), pp: 2255–2258.

[12] J. E. Dominguez, X. Q. Pan, L. Fu, P. A. Van Rompay, Z. Zhang, J. A. Nees, and P. P. Pronko, " Epitaxial SnO_2 thin films grown on .1¯ 012. sapphire by

femtosecond pulsed laser deposition", J. Appl. Phys., Vol. 91, No. 3, 1 February (2002), pp: 1060-1065.
[13] J. E. Dominguez, L. Fu, and X. Q. Pan "Effect of crystal defects on the electrical properties in epitaxial tin dioxide thin films" Appl. Phys. Lett., Vol. 81, No. 27, 30 December (2002), pp: 5163-5170.
[14] Jochan Joseph, Varghese Mathew, Jacob Mathew, K. E. Abraham " Studies on physical properties and carrier conversion of SnO_2: Nd thin films" Turk J Phys, Vol. 33, (2008), pp: 37-47.
[15] Raid A Ismail and Marwa K Abood "Effect of Nd:YAG laser irradiation on the characteristics of porous silicon photodetector" International Nano Letters 2013,3:11.
[16] Ma.Concepción Arenas, Marina Vega, OmarMartÍnez and Oscar H. Salinas, " Nanocrystalline Porous Silicon: Structural, Optical, Electrical and Photovoltaic Properties", Crystalline Silicon – Properties and Uses, ISBN 978-953-307-587-7, www.intechopen.com, Edited by Prof. Sukumar Basu, 2011.
[17] Hubarevich, Yu, HY, Wang, F, Sun, XW, Smirnov, A: Thin porous silicon fabricated by electrochemical etching in novel ammonium fluoride solution for optoelectronic applications., pp. 14–16 Photonics Global Conference, Singapore (**2010**)
[18] P. N. Patel, V. Mishra, A. K. Panchal, Synthesis and characterization of nano scale porous silicon photonic crystals for optical device and sensing applications, Journal of Optoelectronics and Biomedical Materials Vol. 4 Issue 1, January - March 2012 p. 19 - 28
[19] Hubarevich, Yu, HY, Wang, F, Sun, XW, Smirnov, A: Thin porous silicon fabricated by electrochemical etching in novel ammonium fluoride solution for optoelectronic applications., pp. 14–16 Photonics Global Conference, Singapore (2010)
[20] Bisi, O, Ossicini, S, Pavesi, L: Porous silicon: a quantum sponge structure for silicon based optoelectronics. Surf. Sci. Rep. 38, 1 (2000).
[21] Raid A. Ismail, Journal of Semiconductor Technology and Science. Vol.9, No.1. , March (2009)
[22] Khaldun A. Salman, Z. Hassan, Khalid Omar, Int. J. Electrochem. Sci., 7 , 376 -386, (2012).